Published in final edited form as:
J Mol Cell Cardiol. 2011 March ; 50(3): 460–470. doi:10.1016/j.yjmcc.2010.11.012.

Calcium Influx through Cav1.2 Is a Proximal Signal for Pathological Cardiomyocyte Hypertrophy

Xiongwen Chen[*,1], **Hiroyuki Nakayama**[#,1], **Xiaoying Zhang**[*], **Xiaojie Ai**[*,$], **David M. Harris**[&], **Mingxin Tang**[*], **Hongyu Zhang**[*], **Christopher Szeto**[*], **Kathryn Stockbower**[*], **Remus M. Berretta**[*], **Andrea D. Eckhart**[&], **Walter J. Koch**[&], **Jeffery D. Molkentin**[#], and **Steven R. Houser**[*]

[*] Cardiovascular Research Center & Department of Physiology, Temple University School of Medicine, Philadelphia, PA 19140

[#] Cincinnati Children's Hospital Medical Center, University of Cincinnati, Cincinnati, OH 45229

[$] School of Agriculture and Biology, Shanghai Jiao Tong University, Shanghai 200240, P. R. China

[&] Center for Translational Medicine, Thomas Jefferson University, Philadelphia, PA 19107

Abstract

Pathological cardiac hypertrophy (PCH) is associated with the development of arrhythmia and congestive heart failure. While calcium (Ca^{2+}) is implicated in hypertrophic signaling pathways, the specific role of Ca^{2+} influx through the L-type Ca^{2+} channel ($I_{Ca\text{-}L}$) has been controversial and is the topic of this study. To determine if and how sustained increases in $I_{Ca\text{-}L}$ induces PCH, transgenic mouse models with low (LE) and high (HE) expression levels of the β2a subunit of Ca^{2+} channels (β2a) and in cultured adult feline (AF) and neonatal rat (NR) ventricular myocytes (VMs) infected with an adenovirus containing a β2a-GFP.

Results—*In vivo*, β2a LE and HE mice had increased heart weight to body weight ratio, posterior wall and interventricular septal thickness, tissue fibrosis, myocyte volume and cross sectional area and the expression of PCH markers in a time- and dose- dependent manner. PCH was associated with a hypercontractile phenotype including enhanced $I_{Ca\text{-}L}$, fractional shortening, peak Ca^{2+} transient, at the myocyte level, greater ejection fraction and fractional shortening at the organ level. In addition, LE mice had an exaggerated hypertrophic response to transverse aortic constriction. *In vitro* overexpression of β2a in cultured AFVMs increased $I_{Ca\text{-}L}$, cell volume, protein synthesis, NFAT and HDAC translocations and in NRVMs increased surface area. These effects were abolished by the blockade of $I_{Ca\text{-}L}$, intracellular Ca^{2+}, calcineurin, CaMK II and SERCA.

Conclusion—Increasing $I_{Ca\text{-}L}$ is sufficient to induce PCH through the calcineurin/NFAT and CaMKII/HDAC pathways. Both cytosolic and SR/ER-nuclear envelop Ca^{2+} pools were shown to be involved.

Address all correspondence to XC and SRH at the addresses above: Phone 215-707-3542 or 215-7073278, Fax 215-707-5737, xchen001@temple.edu; srhouser@temple.edu.
[1]These two authors contribute equally to this study.

Disclosures: None.

Keywords

L-type calcium channel (or Cav1.2); β_{2a} subunit; Ventricular Myocyte; hypertrophy; transgenic mouse

Introduction

Pathological cardiac hypertrophy (PCH) is an independent risk factor for myocardial infarction, arrhythmia, and subsequent heart failure [1]. It occurs in response to hemodynamic stress such as hypertension, myocardial infarction (MI) and vavular diseases [1]. Pathological cardiovascular stress increases the contractility demands of the heart and its resident myocytes, which is achieved by activating the sympathetic nervous system [2]. Sympathetic neurohormones activate protein kinas A (PKA) to increase Ca^{2+} influx, SR Ca^{2+} uptake, storage, and release to increase the amplitude of the systolic Ca^{2+} transients and contractility [3]. Persistent activation of these signaling pathways also activates Ca^{2+}/calmodulin dependent kinases (CaMK) which is associated with PCH [4].

Ca^{2+} regulates many hypertrophic pathways and well known examples are the Ca^{2+}-regulated calcineurin/NFAT and CaMK/HDAC pathways [1]. However, the proximal source of Ca^{2+} that induces PCH is still not well understood. Ca^{2+} influxes through the Cav1.2/L-type Ca^{2+} channels ($I_{Ca\text{-}L}$) [5–7], Cav3.2/α1H T-type Ca^{2+} channels [8], and transient receptor potential channels (TRPC) [9] have all been proposed to contribute to the pool of Ca^{2+} that activates hypertrophic pathways. In cardiac myocytes, $I_{Ca\text{-}L}$ is the major Ca^{2+} influx and under physiological condition, $I_{Ca\text{-}L}$ does not activate PCH. Under pathological conditions, activated neurohumoral systems increase $I_{Ca\text{-}L}$ which is a likely source of Ca^{2+} to regulate hypertrophic signaling in vivo. This idea is supported by those studies that have shown a necessary role of enhanced $I_{Ca\text{-}L}$ for the myocyte hypertrophy induced by phenylephrine (PE) [10], endothelin-1 (ET-1) [11], isoproterenol [12], angiotensin II [9], elevated extracellular KCl [13] and stretch [14]. $I_{Ca\text{-}L}$ is also able to activate key hypertrophic signaling molecules such as PKC [15] in cardiomyocytes. Cav1.2 channel blockers have been shown to reduce cardiac hypertrophy [6,16] but the exact mechanism is not clear. More recently, it has been shown that reducing the expression of the Cavβ gene decreases $I_{Ca\text{-}L}$ and blunts hypertrophy induced by transverse aortic constriction (TAC) in adult rats [10]. *We have also shown that Cavβ2a overexpression leads to cardiac hypertrophy at the age of 4 months when heart failure phenotype is present in the HE mice* [17]. Other Ca^{2+} influx pathways also seem to be a source of hypertrophic Ca^{2+}, since the loss of Cav3.2/α1H [8] or TRPCs [18] blunts cardiac hypertrophy induced by TAC. Therefore, different routes of Ca^{2+} influx may synergically serve as the source for myocyte hypertrophy [19]. The fact that Cav3.1/α1G overexpression in the mice is antihypertrophic rather than prohypertrophic show the complex nature of Ca^{2+} mediated induction of PCH.

We used transgenic mice with cardiac specific overexpression of the β_{2a}subunit of the L-type Ca2+ channel and cultured adult feline ventricular myocytes (AFVM) and neonatal rat ventricular myocytes (NRVM) with enhanced $I_{Ca\text{-}L}$ by overexpressing the β_{2a} subunit to: (1), determine whether increased $I_{Ca\text{-}L}$ was sufficient to induce myocyte hypertrophy; (2) test if enhanced $I_{Ca\text{-}L}$ could exacerbate PCH induced by TAC; and (3) determine the signaling cascades for myocyte hypertrophy induced by enhanced $I_{Ca\text{-}L}$. Our results show that increasing $I_{Ca\text{-}L}$ is sufficient to induce myocyte hypertrophy by activation of the calcineurin/NFAT and CaMK II/HDAC signaling pathways. Both cytosolic and SR/ER-nuclear envelop Ca^{2+} pools were shown to be involved.

Materials and Methods

Transgenic (TG) mice overexpressing Cavβ2a (β2a)

Cardiac myocytes specific (α-MHC promoter) with inducible (tetracycline-activator (tTA)) β2a mouse lines with high (HE) and low expression (LE) levels were established [17,20]. β2a increases the open probability and membrane trafficking of the pore-forming Cav1.2α1c subunit. Mice with both β2a and tTA transgenes (double transgenic, DTG) and off doxycycline (DOX, a derivative of tetracycline) were used as the experimental group and mice with single transgene (STG) or no transgene (wild-type, WT) were used as controls (Ctr). *Since our previous study has shown that HE mice develop heart failure with associated hypertrophy at the age of 4 months (4m), we used 3-month (3m) old Cavβ_{2a} HE mice to avoid the possibility that PCH in HE was secondary to heart failure. LE mice were used at the age of 4 months. The controls for HE and LE were 3-month old FVB and 4-month old FVB mice, respectively. Our preliminary studies showed that there was no difference in most of the measured parameters between 3m old and 4m old FVB control mice and thus those measurements in these two age groups of controls were pooled.* The investigation conformed to the NIH *Guide for the Care and Use of Laboratory Animals* and was approved by the Institutional Animal Care and Use Committee at Temple University.

Western blotting

To quantitate the expression and phosphorylation of the major Ca^{2+} handling proteins in the animal hearts or cultured myocytes, standard Western blot procedures were performed with antibodies against GAPDH, phospholamban (PLB), phosphorylated PLB at ser16 (pSer16-PLB), phosphorylated PLB at threonine17 (pThr17 PLB), Na^{+}/Ca^{2+} exchange 1 (NCX1), sarcoplasmic/endoplasmic reticulum Ca^{2+}-ATPase 2a (SERCA2a), Cav1.2α1c, and ryanodine receptor type 2 (RyR2). The antibodies were purchased from Millipore (PLB, α1c and NCX1), Badrilla Ltd. (pSer16PLB and pThr17 PLB), and Sigma (SERCA2a and GAPDH), respectively. Immunoblots were visualized with a chemiluminescent reagent (Lumigen PS-3, GE Healthcare UK Ltd., UK) and a Fujifilm LAS-4000 imaging system (Fujifilm Life Science USA). The target proteins were then analyzed with the Multi Gauge software (Fujifilm Life Science USA). The amount of the proteins were normalized to the internal control, GAPDH. The phosphorylation levels of PLB were evaluated by normalizing the phosphorylated PLB to the total PLB amount.

Myocyte isolation, culture and transfection with adenoviruses

Normal adult feline VMs (AFVMs) [21], neonatal rat VMs (NRVMs) [22] and adult mouse VMs [17] were isolated as described previously. Myocytes were cultured and infected with adenoviruses (AdGFP or Adβ_{2a} or AdHDAC and AdNFAT) at the desired multiplicity of infection (MOI) as described previously [21].

Ca^{2+} current, calcium transient, SR Ca^{2+} content and contraction measurements

$I_{Ca\text{-}L}$, cytosolic resting Ca^{2+}, Ca^{2+} transients, *SR Ca^{2+} content*, and myocyte contractions were measured as described previously [21,23].

Myocyte volume, protein/DNA ratio, cell surface area

The increases in the cell volume, protein/DNA ratio and cell surface area are features of myocyte hypertrophy. The volumes of freshly isolated mouse VMs and detached AFVMs that were infected with adenoviruses for 4 days were measured with a Beckman Z2 Coulter Counter [22]. The protein and DNA were isolated from the same sample with Trizol reagent (Invitrogen) and determined with the Biorad RC DC Protein Assay Kit II (Biorad) and a UV

spectrometer, respectively. NRVMs were stained with Rodamine-philloidin (Sigma-Aldrich) for measuring surface area and for sarcomere organization examination.

In vivo cardiac structure and function

Echocardiography (ECHO) was performed with a VisualSonics Vevo 770 machine. Mice were anesthetized with 2% isoflurane initially and then 1% during the ECHO procedure. Hearts were viewed in the short-axis between the two papillary muscles and analyzed in M-mode.

Heart weight to body weight ratio (HW/BW), myocardial fibrosis and myocyte cross sectional area

HW/BW ratios of LE (4m) and HE (3m) mice were measured. Standard histology techniques were used. Five slides from the middle portion of each heart were stained for FITC-labeled lectin (Sigma-Aldrich) and DAPI (Invitrogen) and then imaged. The cross sectional areas of 50 myocytes with round shape and clear nuclei were measured for each slide. To reveal collagen deposition (fibrosis), Mason's trichrome staining was done with tissue sections and fibrotic area was quantitated with ImageJ.

Real-time PCR

Total mRNA was extracted from snap-frozen ventricular tissues using Trizol reagent and quantitated by a UV spectrometer. Real-time PCR was done with the SYBR Green Real Time PCR kit (Applied Biosystems, Carlsbad, CA) and an Eppendorff Mastercycler RT-PCR machine. ANF and β-myosin heavy chain (β-MHC) mRNAs were measured with GAPDH as the internal control. The primers were (5′ to 3′): ANF: forward: tgccggtagaagatgaggtc and reverse: tgcttttcaagagggcagat; β-MHC: forward: acaagctgcagctgaaggtgaa and reverse: aagagctactcctcattcaggccctt; GAPDH: forward: tgcaccaccaactgcttag and reverse: gatgcagggatgatgttc.

Luciferase reporter activity in β2a transgenic mice

β2a transgenic mice were bred with transgenic mice with luciferase reporter gene under the control of NFAT promoter.

Transverse Aortic Constriction (TAC) Model

Cavβ2a LE mice at the age of 6 weeks were used for TAC [17] to avoid any effects of a basal phenotype. Briefly, the transverse aortic arch was visualized through a median sternotomy and 7-0 silk ligation was tied around the aorta with a 26-gauge needle between the right brachiocephalic and left common carotid arteries with subsequent removal of the needle to make the constriction. Hearts were studied 4 weeks following the operation.

Pharmacology

A nonspecific caspase inhibitor, z-VAD-fmk (10μM, BD Biosciences) was used to inhibit myocyte apoptosis when Adβ2a at high MOIs (50 and 100) was used. Inhibitors of Cav1.2 (Nifedipine, 13μM), CaMK II (KN-93 1μM, Sigma), calcineurin (FK 506 (1μM) and Cyclosporine A (CsA, 5μM), Sigma) and sarco/endoplasmic reticulum Ca^{2+}-ATPase (SERCA) (Thapsigargin, TSG, 10nM) were also used.

Statistics

Data in the text are reported as mean±SEM. When appropriate, paired and unpaired T-test, ANOVA or ANOVA for repeated measures were used to detect significance with SAS 9.0

(SAS Institute Inc.). P values of ≤0.05 were considered significant. “n” is the number of cells examined and “N” is the number of cell cultures or the number of animals used.

Results

β2a DTG myocytes have increased $I_{Ca\text{-}L}$ and are hypercontractile

To determine if persistent increases in $I_{Ca\text{-}L}$ can induce PCH *in vivo*, we established DTG lines with low (LE, 3.1 fold) and high (HE, 7.4 fold) β2a expression [17]. Previously we found that the expression of β2a in our DTG mice is stable at about 4m in LE and at 3m in HE mice, when animals were off DOX at weaning (3 weeks) [17]. $I_{Ca\text{-}L}$, myocyte fractional shortening, and Ca^{2+} transients were measured in myocytes isolated from 4m LE or 3m HE mice. $I_{Ca\text{-}L}$ density was greater in β2a-DTG VMs than in controls and was graded with β2a expression (Figure 1A & B). Fractional shortening and Ca^{2+} transient amplitudes (at 0.5Hz) were significantly greater in DTG-VMs, indicating enhanced Ca^{2+} handling (Figure 1C, D & E), *due to increased Ca^{2+} influx and resultant increases in SR Ca^{2+} content (*Figure 1D) that was the highest in the HE myocytes. The diastolic Ca^{2+} was not significantly different between control and DTG myocytes (0.5Hz). *Western analysis was used to quantitate the expression of Ca^{2+} handing proteins: total PLB, pSer16 PLB, pThr17 PLB, SERCA2, RyR2, NCX and α1c. No difference in the expression of these proteins was observed in 3-month and 4- month control mice and thus all the control data were pooled (*Figure 1F and G). No change of the expression of total PLB, pSer16 PLB, NCX, and α1c was found in β2a-DTG LE and HE mice comparing to control mice. The expression of SERCA was increased in HE hearts and pThr17 PLB was increased in both LE and HE hearts, showing that the hypercontractility in LE and HE myocytes is associated with activated CaMKII. The expression of RyR2, was significantly decreased in both LE and HE hearts (Figure 1E and F). These data indicate that there are compensatory changes in some but not all Ca^{2+} *handling proteins in LE and HE hearts with Cavβ2a induced increases in Ca^{2+} influx.*

β2a DTG hearts are hypercontractile and hypertrophied

Ejection fraction (EF) and fractional shortening (FS) were not different at 2m between the three groups but were increased in the HE mice at 3m and in LE mice at 4m (Figure 2B). HE animals developed depressed cardiac EF and FS at 4m which continued to decline at 6m. In the LE mice, EF and FS remained greater than controls at these ages (4m and 6m) (Figure 2C & D). The thicknesses of diastolic left ventricular posterior wall ($LVPW_d$) and anterior/ interventricular septal wall (IVS_d) were not significantly different between the groups at 2m but increased in the LE mice and increased (3m) and then decreased (4–6m) in the HE mice (Figure 2E and F). The left ventricular internal diameter during diastole ($LVID_d$) was not different between the control and LE mice although it tended to be smaller in the LE mice consistent with concentric LV hypertrophy. Diastolic LVID in HE mice continued to increase during the age of 4–6m, indicating LV dilation (Figure 2G). In agreement with the changes in the wall thickness, the LV mass estimated by ECHO increased steadily in the LE and HE mice. The LV mass/BW was the highest in the HE (HE>LE>ctr). (Figure 2H and I).

HW/BW ratios were also directly measured in excised hearts at 3m in HE and 4m in LE mice (Figure 2). At these ages, HW/BW was significantly increased in LE and HE (12.8% and 19.3%) versus control mice (Figure 3B). Ventricular weight to body weight (VW/BW) was increased by 15.7% and 40.9% in LE and HE β2a hearts (Figure 3A & C). At the tissue level, fibrosis (light blue staining in Figure 3D) was observed in the hearts of DTG mice. The cross sectional areas of VMs in LE and HE were 26.9% and 79.6% larger than in controls, respectively (Figure 3E & F). Ventricular myocyte volume was greater in LE (18.7%) and HE (42.8%) versus control mice (Figure 3G). The mRNA expression of PCH markers, ANF and β-MHC, was not significantly different between control and LE mice but

were significantly increased in HE mice at 3m. At 4m, mRNA expression of both genes was increased to similar extents in HE and LE mice (Figure 3H & I). NFAT activity was significantly increased in β2a hearts (Figure 3J). These results show a strong association between β2a induced increases in contractility and cardiac hypertrophy.

β2a transgenic mice have exaggerated hypertrophy after transverse aortic constriction

At the age of 6 weeks, control and LE mice were subjected to transverse aortic constriction (TAC). TAC induced a high mortality in HE (>60%) and these animals were not studied. The initial survival rates for control and LE mice were not different and were about 80~85%. After 4 weeks of TAC, LE mice had greater HW/BW ratio and greater increases in myocyte cross sectional area than controls (Figure 4A&B). LE mice had depressed cardiac pump function evidenced by decreased ejection fraction (Figure 4C) and increased lung weight to body weight ratio, an index of pulmonary edema (Figure 4D). *Similar to isoproterenol infusion as we reported previously* [17], *TAC caused much more severe fibrosis in the LE mice after TAC (*Figure 4E and F).

Ca^{2+} handling in cultured AFVMs after β2a expression

Myocyte hypertrophy in vivo is a complex process. To more directly test the role of β2a and $I_{Ca\text{-}L}$ in myocyte hypertrophy, we employed in vitro AFVM and NRVM culture systems to study the relationship between increased $I_{Ca\text{-}L}$ and myocyte hypertrophy.

Increasing the multiplicity of infections (MOIs, 0, 5, 100) of Adβ2a (AdGFP as the control) graded $I_{Ca\text{-}L}$ in AFVMs at 48 hours post infection (Table 1). The amplitudes of unloaded contractions and Ca^{2+} transients were also enhanced with the increased β_{2a} but diastolic Ca^{2+} was not changed. The SR Ca^{2+} content was significantly increased and was graded with β2a expression. These results show that the Ca^{2+} handling phenotype of β2a mouse myocytes is reproduced in AFVMs infected with Adβ2a.

β2a overexpression induces hypertrophy in vitro

We then tested if VMs infected with β2a were hypertrophied. Myocyte volume and protein synthesis (protein/DNA ratio) were compared in β2a- versus in GFP-AFVMs. GFP overexpression did not have a significant effect on AFVM volume but β2a increased AFVM volume in an Adβ2a MOI-dependent fashion (Figure 5A). The increases in myocyte volume induced by β2a overexpression were 10% to 20% (Figure 5B). Adβ2a infection of AFVM at an MOI of 5 caused protein/DNA ratio to increase by 33.8±7.0% (Figure 5C) compared to AdGFP. β2a infection of NRVMs (1123.5±30.1μm^2) increased NRVM surface area (52.4%) more than AdGFP (737.0±23.9μm^2) and induced more organized sarcomeres (Figure 5D). These data suggest that increases in Ca^{2+} influx through Cav1.2 induce cardiac myocyte hypertrophy.

β2a causes NFAT3 and HDAC5 translocation

We tested whether the pathways involving calcineurin (CaN)/NFAT3 and the CaMK II/HDAC5 were activated. AFVMs were co-infected with adenoviruses containing an NFATc4 (NFAT3)-GFP fusion gene (MOI=100) or an HDAC5-GFP (MOI=100) fusion gene and Adβ2a (MOI=5) or AdGFP (MOI=5). The GFP fluorescence from AdGFP or Adβ2a was weak at 48 hours post infection and did not interfere with the strong NFAT-GFP and HDAC-GFP fluorescence. Co-infection with AdNFAT-GFP and AdGFP resulted in strong fluorescence that was evenly distributed in the cytoplasm of AFVMs (Figure 6A) and some AFVMs with slightly green nuclei *like in some of GFP-AFVMs, possibly due to baseline CaN activity*. In AFVMs co-infected with both Adβ2a and AdNFAT3, the majority VMs had

bright green nuclei (Figure 6B & C). These results show that the CaN/NFAT3 pathway is activated after increased Ca^{2+} influx.

HDAC, a repressor of hypertrophic signaling, is found in the nucleus under basal conditions and translocates into the cytosol when it is phosphorylated by CaMK II or other kinases. The % of AFVMs in which HDAC5 was translocated to the cytoplasm (% of nuclei without HDAC5) was significantly higher in β_{2a}-AFVMs than in GFP-AFVMs (Figure 6D, E & F). *Increased CaMK II activity may be responsible for the HDAC5 translocation from the nucleus in β2a infected myocytes, as indicated by the increased PLB phosphorylation at Thr17*. (Figure 6G).

β_{2a}-induced myocyte hypertrophy involves CaN and CaMK II activation

Treatments of β2a -AFVMs with a Cav1.2 blocker (nifedipine, 10μM), an intracellular Ca^{2+} buffer (BAPTA-AM, 1μM), CaN inhibitors (CsA, 5μM and FK 506, 1μM), and a CaMK II inhibitor (KN93, 1μM), all prevented β2a-induced increases in myocyte volume (Figure 7A), protein/DNA ratio (Figure 7B) and β2a-induced NFAT translocation (Figure 7C). Similarly, inhibition of CaMK II with KN93 abolished the HDAC5 translocation induced by β2a (Figure 7D). These results suggest that the myocyte hypertrophy observed in β2a-myocytes is mediated by increases in Ca^{2+} influx and subsequent activation of CaN/NFAT and CaMK II/HDAC signaling pathways.

Phenylephrine (PE), a hypertrophic agonist, increased myocyte volume, NFAT and HDAC translocation in AFVMs (Figure 7) infected with both Adβ2a and AdGFP. However, phenylephrine did not further increase these hypertrophic parameters in β2a-AFVMs.

SR Ca^{2+} may be involved in myocyte hypertrophy by providing local release of Ca^{2+} from the perinuclear envelope into the nucleus to induce HDAC translocation [24] and/or by releasing Ca^{2+} into the cytoplasm [13]. Inhibiting SERCA with thapsigargin (TSG) significantly increased diastolic Ca^{2+} and reduced SR Ca^{2+} content in both GFP and β2a-VMs (Table 1). TSG also abolished Ca^{2+} transients in cultured myocytes. It also blocked β2a-induced myocyte hypertrophy (Figure 7A and B) and the translocation of HDAC from the nucleus to the cytoplasm (Figure 7D). However, TSG did not block NFAT translocation in β2a-AFVMs (Figure 7C) and in GFP-AFVMs TSG promoted NFAT nuclear translocation without inducing hypertrophy. These data suggest that SR Ca^{2+} is necessary for β2a-mediated HDAC translocation and hypertrophy but not necessary for NFAT translocation.

Discussion

Increases in myocyte [Ca^{2+}] induce PCH [8,13,25], but the source of the hypertrophic [Ca^{2+}] are still not clearly defined. The conundrum is that myocyte cytosolic [Ca^{2+}] fluctuates over a wide range during each normal heart beat, and can be increased with physiological stimuli such as exercise and pregnancy without inducing PCH [1]. In the present study we tested the idea that persistent increases in $I_{Ca\text{-}L}$, the primary Ca^{2+} influx pathway in the heart, are sufficient to cause PCH. Our experiments showed that persistent increases in Ca^{2+} influx caused enhanced contractions and Ca^{2+} transients and these changes were associated with myocyte hypertrophy, both *in-vitro* and *in-vivo*, indicating a direct effect of increased Ca^{2+} influx on myocyte hypertrophy. We also showed that both NFAT and HDAC nuclear translocation were necessary for LTCC-dependent hypertrophy. NFAT translocation is more dependent on the change of cytosolic Ca^{2+} while HDAC translocation is more related to the increase of SR-nuclear envelope Ca^{2+}.

Is increased Ca^{2+} influx through Cav1.2 inducing pathological hypertrophy?

Previously, we have shown that Cavβ2a DTG mice develop cardiac hypertrophy associated cardiac arrhythmia [26] and premature death [17], fibrosis, blunted β-adrenergic responses and diastolic dysfunction when stressed [23]. Here we show that in the DTG hearts the expression of markers of pathological hypertrophy, ANF and β-MHC, are increased. These features of Cavβ2a DTG hearts indicate that the hearts of Cavβ2a DTG mice are more likely to have pathological hypertrophy. However, whether Cavβ2a LE and HE hearts undergo decompensation is depending on the extent of SR and cytosolic Ca^{2+} overload because LE mouse hearts remain hypercontractile up to one year while HE mice develop heart failure after the age of 4 months. Furthermore, we are not clear whether the pathological hypertrophy was secondary to myocyte apoptosis or necrosis induced by mitochondrial Ca^{2+}-overload.

Sources of "hypertrophic Ca^{2+}"?

Persistent changes in the amplitude and duration of the systolic [Ca^{2+}] transient that are specific to pathological stress could activate induce pathological hypertrophy signaling. There is reasonable evidence for this hypothesis [13]. Our results show that persistently increasing Ca^{2+} influx through Cav1.2 increases the Ca^{2+} transient amplitude and diastolic Ca^{2+} at high contracting rates and activate the signaling cascades to induce pathological hypertrophy. Consistent with our study, it has been shown that LTCC blockers eliminate NRVM hypertrophy induced by many neurohormones [9–13] and stretch [14]. In vivo, there is also evidence that reducing the increase in Ca^{2+} influx through Cav1.2 by knockdown of the β2 subunit [10] or with Ca^{2+} channel blockers (benidipine) [7] after pressure overload reduces the ensuing hypertrophy. Whether increased Ca^{2+} influx through Cav1.2 induces cardiac hypertrophy by enhancing contractile Ca^{2+} transients or through a local domain (e.g., calveolae) is not yet clear.

Some studies suggest that the source of Ca^{2+} for activation of hypertrophic signaling is distinct from the Ca^{2+} that activates myofilaments [25]. These sources of hypertrophic Ca^{2+} include Ca^{2+} entry through T-type Ca^{2+} channels (TTCC) [8], TRP channels [9,27] or capacitive Ca^{2+} entry [28]. Many years ago we postulated that the re-expression of TTCC in diseased hearts might play a role in hypertrophic signaling [29]. A recent report addressing this hypothesis suggests that in pressure overload, hypertrophic Ca^{2+} enters myocytes exclusively through α1H TTCC [8]. These studies suggest that hypertrophic Ca^{2+} entry is compartmentalized to activate PCH signaling independent of changes in bulk cytoplasmic [Ca^{2+}]. However, not all enhanced Ca^{2+} influx is able to induce PCH. We have shown that enhanced Ca^{2+} influx through the Cav3.1 (α1G) TTCC does not induce PCH and actually antagonizes cardiac hypertrophy induced by TAC [30].

There is some evidence that the [Ca^{2+}] released from the nuclear envelope, which is contiguous with the SR, through IP3 receptors activates the CaMK/HDAC pathway [24,31] to activate hypertrophic signaling. Activation of IP3 receptors may be independent of the cytoplasmic [Ca^{2+}] transient and may require activation of membrane receptors by prohypertrophic neurohormones such as angiotensin and endothelin [31]. Our study shows that the β2a-VMs have increased SR Ca^{2+} content and suggests that this could be involved in induction of pathological hypertrophy. Future studies will need to resolve the role of microdomain signaling and Ca^{2+} loading of the SR-nuclear envelope in β2a-induced hypertrophy.

Ca^{2+} mediated hypertrophic signaling cascades

Hypertrophic pathways including CaN/NFAT, CaMKII/HDAC, PKC, and MAPK pathways are regulated by Ca^{2+} [1]. We found that both the CaN/NFAT and CaMKII/HDAC

pathways are activated when Ca^{2+} influx is increased and that inhibiting these two pathways prevented Ca^{2+}-mediated myocyte hypertrophy *in vitro*. We also explored the potential involvement of these pathways *in vivo* by using NFAT activity reporter mice and measuring CaMK II activity. All studies suggest a critical role for CaN/NFAT and CaMKII/HDAC pathways signaling cascades in PCH induced by β2a.

How is the hypertrophic [Ca^{2+}] signal at the surface membrane transduced to the nucleus?

Our data suggest that the SR could be a primary sensor of cell stress and changes in SR [Ca^{2+}] are necessary for activation of both cytoplasmic and nuclear prohypertrophic signals. Persistent increases in Ca^{2+} influx will increase SR Ca^{2+} loading and release to provide the local cytoplasmic [Ca^{2+}] required for activation of hypertrophic signaling. Since the nuclear envelope is contiguous with the SR, increasing SR Ca^{2+} may result in an increase in nuclear Ca^{2+} transients and thereafter activation of nuclear hypertrophic signaling. We used thapsigargin to inhibit SERCA *and abolish SR Ca^{2+} uptake and subsequent SR Ca^{2+} release*. This treatment blocked β2a-induced hypertrophy and HDAC translocation, but initiated NFAT nuclear translocation. These results suggest that elevated cytoplasmic [Ca^{2+}] by thapsigargin activates CaN/NFAT signaling without activating nuclear CaMKII/HDAC signaling. *However, we could not determine whether the blunted myocyte hypertrophy by TSG is due to the abolishment of Ca^{2+} transients or compartmented SR/nuclear envelope Ca^{2+} release. It is likely that the elimination of nuclear envelope Ca^{2+} release reduced CaMK II activation in the nucleus.* These results also show that at least under our conditions, NFAT and HDAC translocation can be independently controlled and both molecules must be translocated for induction of PCH. *Our results support a role of HDAC as a repressor of PCH and suggest it must be exported from the nucleus for NFAT to initiate hypertrophic responses.* Our study does leave open the possibility that Cav1.2 directly activates calcineurin closely associated with Cav1.2 to induce NFAT translocation [5] *and TSG activates other signaling pathways such as ER stress signaling that may blunt myocyte hypertrophy*.

Ca^{2+} mediated cardiac hypertrophy in human disease

The role of Ca^{2+} influx through Cav1.2 in the induction of PCH in human diseases such as chronic hypertension or after myocardial infarction is unclear. In both of these diseases, systolic wall stress and cardiac myocyte contractility are augmented by enhancing Ca^{2+} influx and subsequent Ca^{2+} handling. The surviving myocardium after myocardial infarction is hypercontractile [32], in large part due to the activated sympathetic system [2]. In addition, β2a expression has been reported to be increased in failing human hearts [33]. These studies suggest that increases in Ca^{2+} entry may be a proximal cause of the PCH in humans. This is difficult to prove because LTCC antagonists usually affect the vasculature and systolic blood pressure before cardiac effects are observed [34]. However, there are many clinical scenarios in which Ca^{2+} channel antagonists are used and regression of cardiac hypertrophy is induced [34].

Conclusion

Our studies suggest that excessive Ca^{2+} influx through Cav1.2 is a proximal source of Ca^{2+} for pathological hypertrophy.

Research Highlights

Calcium (Ca) is a necessary signaling molecule for activating hypertrophic responses. However the source(s) of the proximal Ca is not clear yet. This study aims to explore whether persistently enhanced Ca influx through the L-type Ca channel (Cav1.2), a

situation happening when the heart is stressed, is sufficient to induce pathological cardiac hypertrophy and what is the underlying mechanism. The highlights in this study include:

1. We used in-vivo transgenic mouse systems and in vitro cell culture systems overexpressing the Cavβ2a subunit to persistently increase Ca influx through Cav1.2 to make a complete study showing that persistently increasing Ca influx through Cav1.2 is sufficient to induce cardiac hypertrophy both in vivo and in vitro and the underlying mechanisms involve calcineurin/NFAT and CaMK II/HDAC pathways. Therefore, enhanced Ca influx through Cav1.2 could be a more pathologically relevant proximal Ca influx for cardiac hypertrophy.
2. The in vivo transgenic mouse systems include a low expression line and a high expression line, which makes the study of the effect of gene doses possible. Our study show that the higher the expression of Cavβ2a, the more Ca influx and more severe cardiac hypertrophy.
3. The study of these transgenic mouse lines is serial, revealing the progression of cardiac hypertrophy. We show the development of hypercontractile and compensated hypertrophy first then decompensation/heart failure in the high expression mouse line. In the low expression line, the mice do not develop heart failure during the study period. No comparable results from these mouse lines have been published.
4. The enhanced hypertrophic response to TAC in mice with increased Ca influx has not been reported to date.
5. In vitro cell culture systems include both adult feline ventricular myocytes and neonatal rat ventricular myocytes. In both systems, Cavβ2a expression induces myocyte hypertrophy in a gene-dose-dependent manner, suggesting a universal phenotype. Careful evaluation of Ca handling and myocyte hypertrophy has been done. No similar study has been reported so far.
6. Our study shows that the underlying mechanism involves the two Ca-activated signaling pathways: CaN/NFAT and CaMK II/HDAC pathways. It is possible that different pools of Ca activate these two pathways: cytosolic Ca activates CaN/NFAT pathway while SR-nuclear envelope Ca release activates CaMK II/HDAC pathway. These are novel findings.

Acknowledgments

Funding:

This work was supported by grants from the NIH (HL089312 to SRH and HL088243 to XC); HHMI (to JDM) and American Heart Association (AHA0730347N to XC).

References

1. Heineke J, Molkentin JD. Regulation of cardiac hypertrophy by intracellular signalling pathways. Nat Rev Mol Cell Biol 2006 Aug;7(8):589–600. [PubMed: 16936699]
2. Bristow MR, Kantrowitz NE, Ginsburg R, Fowler MB. Beta-adrenergic function in heart muscle disease and heart failure. J Mol Cell Cardiol 1985 Jul;17(Suppl 2):41–52. [PubMed: 2863387]
3. Dorn GW 2nd. Adrenergic pathways and left ventricular remodeling. J Card Fail 2002 Dec;8(6 Suppl):S370–3. [PubMed: 12555147]
4. Zhang R, Khoo MS, Wu Y, Yang Y, Grueter CE, Ni G, et al. Calmodulin kinase II inhibition protects against structural heart disease. Nat Med 2005 Apr;11(4):409–17. [PubMed: 15793582]

5. Tandan S, Wang Y, Wang TT, Jiang N, Hall DD, Hell JW, et al. Physical and functional interaction between calcineurin and the cardiac L-type Ca2+ channel. Circulation research 2009 Jul 2;105(1): 51–60. [PubMed: 19478199]
6. Semsarian C, Ahmad I, Giewat M, Georgakopoulos D, Schmitt JP, McConnell BK, et al. The L-type calcium channel inhibitor diltiazem prevents cardiomyopathy in a mouse model. The Journal of clinical investigation 2002 Apr;109(8):1013–20. [PubMed: 11956238]
7. Liao Y, Asakura M, Takashima S, Ogai A, Asano Y, Asanuma H, et al. Benidipine, a long-acting calcium channel blocker, inhibits cardiac remodeling in pressure-overloaded mice. Cardiovasc Res 2005 Mar 1;65(4):879–88. [PubMed: 15721868]
8. Chiang CS, Huang CH, Chieng H, Chang YT, Chang D, Chen JJ, et al. The Ca(v)3.2 T-type Ca(2+) channel is required for pressure overload-induced cardiac hypertrophy in mice. Circulation research 2009 Feb 27;104(4):522–30. [PubMed: 19122177]
9. Onohara N, Nishida M, Inoue R, Kobayashi H, Sumimoto H, Sato Y, et al. TRPC3 and TRPC6 are essential for angiotensin II-induced cardiac hypertrophy. Embo J 2006 Nov 15;25(22):5305–16. [PubMed: 17082763]
10. Cingolani E, Ramirez Correa GA, Kizana E, Murata M, Cho HC, Marban E. Gene therapy to inhibit the calcium channel beta subunit: physiological consequences and pathophysiological effects in models of cardiac hypertrophy. Circulation research 2007 Jul 20;101(2):166–75. [PubMed: 17556655]
11. Ikeda K, Tojo K, Tokudome G, Akashi T, Hosoya T, Harada M, et al. Possible involvement of endothelin-1 in cardioprotective effects of benidipine. Hypertens Res 2000 Sep;23(5):491–6. [PubMed: 11016804]
12. Zou Y, Yamazaki T, Nakagawa K, Yamada H, Iriguchi N, Toko H, et al. Continuous blockade of L-type Ca2+ channels suppresses activation of calcineurin and development of cardiac hypertrophy in spontaneously hypertensive rats. Hypertens Res 2002 Jan;25(1):117–24. [PubMed: 11924717]
13. Colella M, Grisan F, Robert V, Turner JD, Thomas AP, Pozzan T. Ca2+ oscillation frequency decoding in cardiac cell hypertrophy: role of calcineurin/NFAT as Ca2+ signal integrators. Proc Natl Acad Sci U S A 2008 Feb 26;105(8):2859–64. [PubMed: 18287024]
14. Zobel C, Rana OR, Saygili E, Bolck B, Saygili E, Diedrichs H, et al. Mechanisms of Ca2+-dependent calcineurin activation in mechanical stretch-induced hypertrophy. Cardiology 2007;107(4):281–90. [PubMed: 17264507]
15. Muth JN, Bodi I, Lewis W, Varadi G, Schwartz A. A Ca(2+)-dependent transgenic model of cardiac hypertrophy: A role for protein kinase Calpha. Circulation 2001 Jan 2;103(1):140–7. [PubMed: 11136699]
16. Huang CY, Hao LY, Buetow DE. Insulin-like growth factor-induced hypertrophy of cultured adult rat cardiomyocytes is L-type calcium-channel-dependent. Molecular and cellular biochemistry 2002 Feb;231(1–2):51–9. [PubMed: 11952165]
17. Nakayama H, Chen X, Baines CP, Klevitsky R, Zhang X, Zhang H, et al. Ca2+- and mitochondrial-dependent cardiomyocyte necrosis as a primary mediator of heart failure. The Journal of clinical investigation 2007 Sep;117(9):2431–44. [PubMed: 17694179]
18. Seth M, Zhang ZS, Mao L, Graham V, Burch J, Stiber J, et al. TRPC1 channels are critical for hypertrophic signaling in the heart. Circulation research 2009 Nov 6;105(10):1023–30. [PubMed: 19797170]
19. Horiba M, Muto T, Ueda N, Opthof T, Miwa K, Hojo M, et al. T-type Ca2+ channel blockers prevent cardiac cell hypertrophy through an inhibition of calcineurin-NFAT3 activation as well as L-type Ca2+ channel blockers. Life sciences 2008 Mar 12;82(11–12):554–60. [PubMed: 18275974]
20. Sanbe A, Gulick J, Hanks MC, Liang Q, Osinska H, Robbins J. Reengineering inducible cardiac-specific transgenesis with an attenuated myosin heavy chain promoter. Circulation research 2003 Apr 4;92(6):609–16. [PubMed: 12623879]
21. Chen X, Zhang X, Kubo H, Harris DM, Mills GD, Moyer J, et al. Ca2+ influx-induced sarcoplasmic reticulum Ca2+ overload causes mitochondrial-dependent apoptosis in ventricular myocytes. Circulation research 2005 Nov 11;97(10):1009–17. [PubMed: 16210547]

22. Chen X, Wilson RM, Kubo H, Berretta RM, Harris DM, Zhang X, et al. Adolescent feline heart contains a population of small, proliferative ventricular myocytes with immature physiological properties. Circulation research 2007 Mar 2;100(4):536–44. [PubMed: 17272809]

23. Tang M, Zhang X, Li Y, Guan Y, Ai X, Szeto C, et al. Enhanced basal contractility but reduced excitation-contraction coupling efficiency and {beta}-adrenergic reserve of hearts with increased Cav1.2 activity. American journal of physiology. Jun 11; (in press).

24. Wu X, Zhang T, Bossuyt J, Li X, McKinsey TA, Dedman JR, et al. Local InsP3-dependent perinuclear Ca2+ signaling in cardiac myocyte excitation-transcription coupling. The Journal of clinical investigation 2006 Mar;116(3):675–82. [PubMed: 16511602]

25. Houser SR, Molkentin JD. Does contractile Ca2+ control calcineurin-NFAT signaling and pathological hypertrophy in cardiac myocytes? Sci Signal 2008;1(25):pe31. [PubMed: 18577756]

26. Tang M, Zhang X, Harris DM, Li Y, Nakayama H, Eckhart A, et al. Enhanced Cav1.2 Influx Induces Cardiac Conduction Disturbances and SR Ca2+ Overload to Induce Cardiac Arrhythmia but With Shortened QT and Action Potentials (Abstract 2733). Circulation 2009;120:S689.

27. Kuwahara K, Wang Y, McAnally J, Richardson JA, Bassel-Duby R, Hill JA, et al. TRPC6 fulfills a calcineurin signaling circuit during pathologic cardiac remodeling. The Journal of clinical investigation 2006 Dec;116(12):3114–26. [PubMed: 17099778]

28. Hunton DL, Lucchesi PA, Pang Y, Cheng X, Dell'Italia LJ, Marchase RB. Capacitative calcium entry contributes to nuclear factor of activated T-cells nuclear translocation and hypertrophy in cardiomyocytes. The Journal of biological chemistry 2002 Apr 19;277(16):14266–73. [PubMed: 11827959]

29. Nuss HB, Houser SR. T-type Ca2+ current is expressed in hypertrophied adult feline left ventricular myocytes. Circulation research 1993 Oct;73(4):777–82. [PubMed: 8396509]

30. Nakayama H, Bodi I, Correll RN, Chen X, Lorenz J, Houser SR, et al. alpha1G-dependent T-type Ca2+ current antagonizes cardiac hypertrophy through a NOS3-dependent mechanism in mice. The Journal of clinical investigation 2009 Dec;119(12):3787–96. [PubMed: 19920353]

31. Higazi DR, Fearnley CJ, Drawnel FM, Talasila A, Corps EM, Ritter O, et al. Endothelin-1-stimulated InsP3-induced Ca2+ release is a nexus for hypertrophic signaling in cardiac myocytes. Molecular cell 2009 Feb 27;33(4):472–82. [PubMed: 19250908]

32. Rechavia E, de Silva R, Nihoyannopoulos P, Lammertsma AA, Jones T, Maseri A. Hyperdynamic performance of remote myocardium in acute infarction. Correlation between regional contractile function and myocardial perfusion. Eur Heart J 1995 Dec;16(12):1845–50. [PubMed: 8682017]

33. Hullin R, Matthes J, von Vietinghoff S, Bodi I, Rubio M, D'Souza K, et al. Increased expression of the auxiliary beta(2)-subunit of ventricular L-type Ca(2)+ channels leads to single-channel activity characteristic of heart failure. PloS one 2007;2(3):e292. [PubMed: 17356701]

34. Klingbeil AU, Schneider M, Martus P, Messerli FH, Schmieder RE. A meta-analysis of the effects of treatment on left ventricular mass in essential hypertension. The American journal of medicine 2003 Jul;115(1):41–6. [PubMed: 12867233]

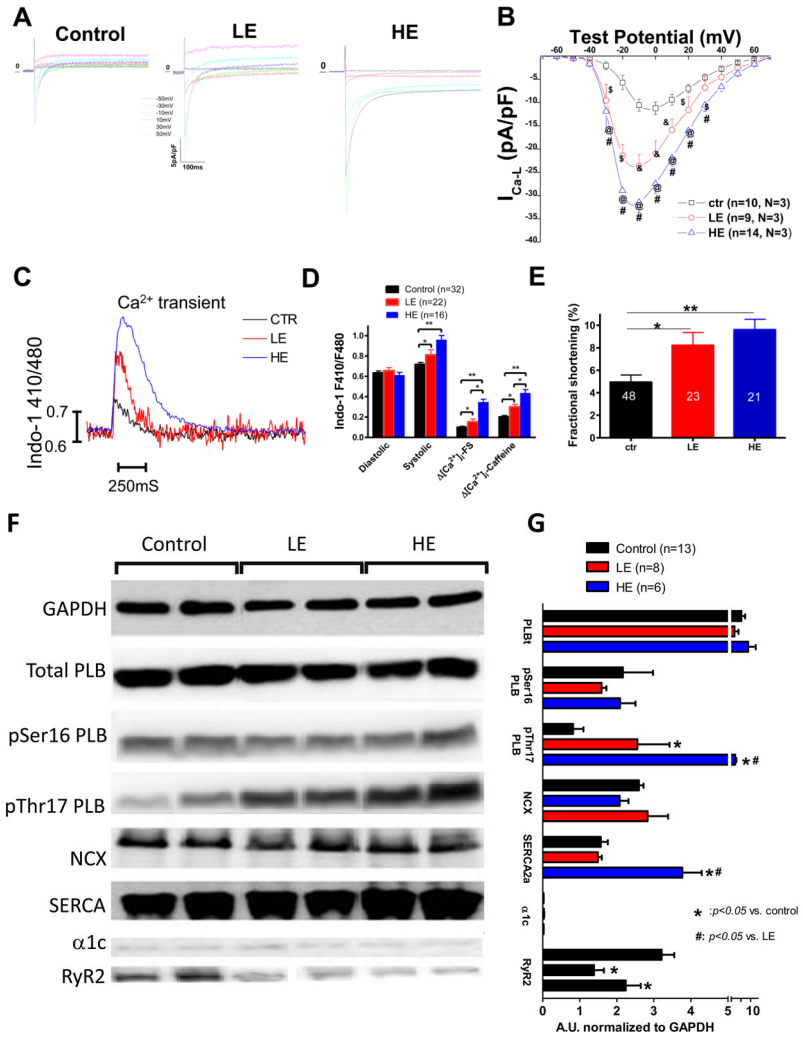

Figure 1. Enhanced Ca^{2+} handling in ventricular myocytes isolated from β2a LE and HE mice

A, examples of I_{Ca-L}. **B**, averaged I–V relationships of I_{Ca-L} in VMs from control (Ctr), LE and HE mice. The maximal I_{Ca-L} in Ctr, LE and HE myocytes were −12.77±0.84, −23.30±2.16, and −33.09±4.01pA/pF, respectively. **C**, Example of Ca^{2+} transients recorded with indo-1 in VMs from Ctr, LE and HE mice (0.5Hz). **D**, There was no difference in diastolic Ca^{2+} in control (0.63±0.02), LE (0.65±0.03) and HE (0.62±0.03) VMs but increased amplitudes of systolic Ca^{2+} in DTG VMs (ctr: 0.72±0.02; LE: 0.81±0.05; HE: 0.96±0.04). **E**, fractional shortening was enhanced β2a (Ctr: 5.0±0.6%; LE: 8.2±1.1%; HE: 9.6±0.9%). ***F***, *Western blots of total PLB, pSer16 PLB, pThr17 PLB, NCX, SERCA, α1c, RyR and GAPDH (internal control) in control, LE and HE heaerts.* ***G***, *Averaged normalized protein expression levels.* In **B**: @: *p<0.01* vs. Ctr; #: *p<0.05* vs. LE; $: *p<0.05* vs. Ctr; &: *p<0.01* vs. Ctr. In **D & E**: *: *p<0.05*; **: *p<0.01*. "n" is the number of cells from at least 3 animals.

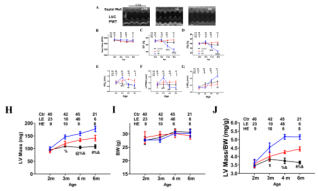

Figure 2. Cardiac hypertrophy in DTG mice

A, Examples of M-mode echocardiography images of Ctr (4-month old), LE (4-month old) and HE (3-month old) mice. **B**, Heart rates were not different between groups when cardiac function was evaluated by echocardiography. **C & D**, Cardiac EF and FS in Ctr, β2a LE and HE mice at 2m–6m. **E & F,** Diastolic IVS and LVPW thickness were increased in both LE and HE mice at 3m but decreased in HE mice at 4m and 6m. IVSd and LVPWd in LE mice remained greater at 4m and 6m. **G**, Diastolic LVID was increased in HE mice at 4m and 6m. **H**, LV masses in LE and HE mice kept increasing from 3m to 6m. **I**, No significant differences in BW were detected between groups. **J**, LV Mass to body weight ratios were increased in LE and HE mice after 3m. # P<0.05 between LE and Ctr; $ P<0.05 between HE and Ctr; & P<0.01 HE vs. LE; @ P<0.001 Ctr vs. LE; % P<0.001 Ctr vs. HE; ! P<0.001 LE vs. HE; * P<0.001 LE vs. HE.

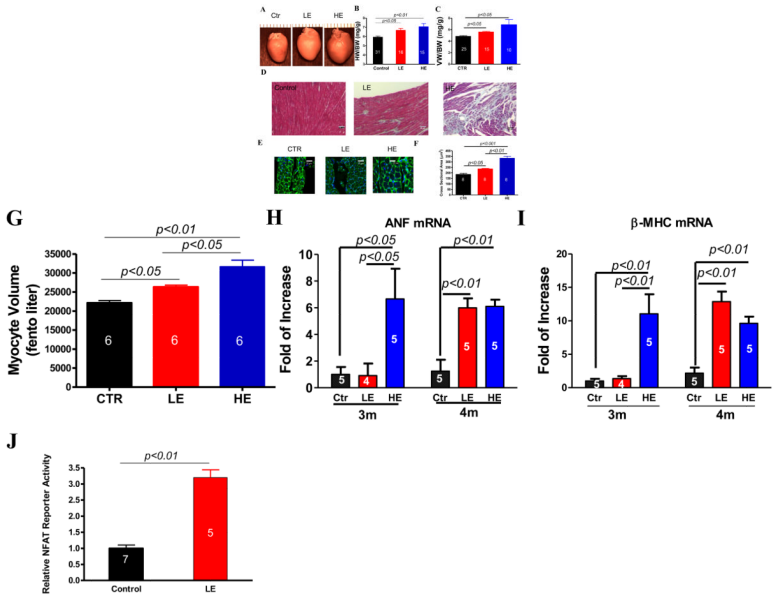

Figure 3. HE and LE mice develops PCH

A, Micrographs of Ctr (4 month), LE (4m) and HE (3m) hearts. The smallest division on the scale bar is 1mm. **B**, HW/BW ratios were significantly greater in LE (6.67±0.22mg/g) and HE (7.06±0.35mg/g) mice than in control (5.92±0.13mg/g) mice. **C**, VW/BW ratios were significantly greater in LE (5.63±0.11mg/g) and HE (6.86±0.90mg/g) mice than in control (4.86±0.11mg/g). **D**, Trichrome-staining of cardiac tissues from Ctr, LE and HE mice showed significant fibrosis (light blue staining) in LE and HE mice. **E**, Example images of lectin-stained cardiac tissue showing cross-sections of myocytes. Green, lectin-stained membrane; Blue: DAPI-stained nuclei. **F**, There were greater cross sectional areas of VMs in HE (334.1±16.5 μm^2) mouse hearts than in control (186.1±9.7 μm^2) and LE (236.0±5.3μm^2) mouse hearts. **G**, VM volume was significantly larger in HE (31,660±1,723fL) than in LE (26,309±503fL) and control mice (22,165±585fL). **H & I**, ANF- and β-MHC- mRNA expression evaluated by real-time PCR. **J**, Relative NFAT activity in DTG myocytes is significantly higher than in control myocytes. One-way ANOVA was done for B, C, F and G, two-way ANOVA for H and I and student t-test for J. The number in the bars indicates the number of hearts examined.

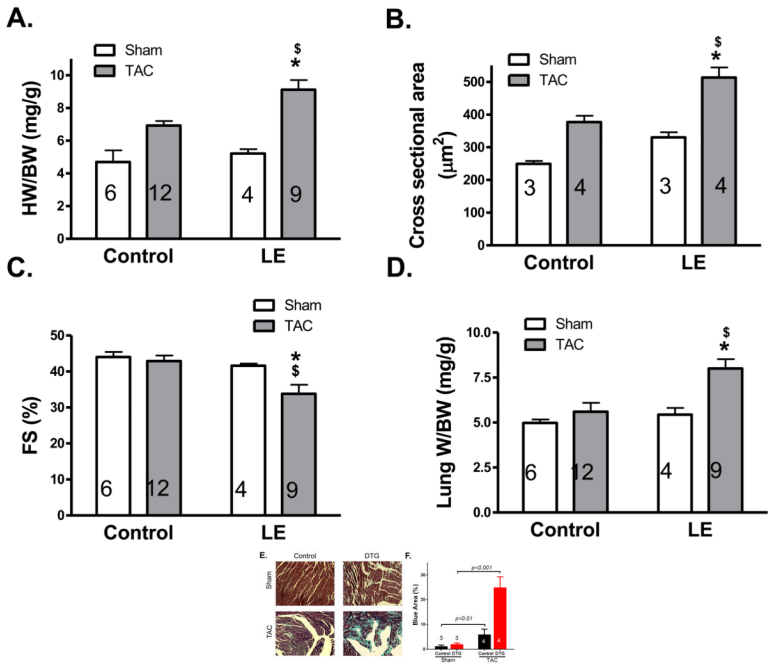

Figure 4. Increases in $I_{Ca\text{-}L}$ promoted hypertrophic response to transverse aortic constriction (TAC)

LE mice developed more severe hypertrophy (**A**) and had increased myocyte cross sectional area (**B**) after TAC. $: *p<0.05* vs. LE sham; *: *p<0.05* vs. control with TAC. **C & D**, The fractional shortening of the heart was reduced and the lung weight to body weight was increased in the LE mice but not in control mice after TAC, indicating the development of heart failure in LE mice. ***E & F***, *raw images and averaged percentage of blue fibrotic area of Mason's Trichrome staining of LV tissues of control and LE mice with (TAC) or without TAC (sham) procedure.*

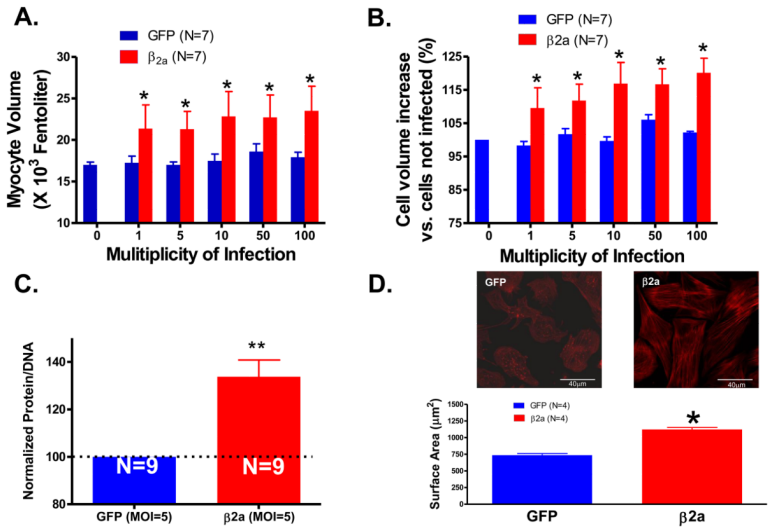

Figure 5. β2a overexpression induces hypertrophy of AFVMs and NRVMs

A & B, The effects of different MOIs (0, 5, 10, 50 and 100) of Adβ2a or AdGFP on myocyte volume. β2a expression significantly increased the volume of AFVMs after 4 days of culture. **C**, Normalized protein/DNA ratio in cells infected with Adβ2a or AdGFP at the MOI of 5. **D**, The effects of Adβ2a (MOI 5) or AdGFP (MOI 5) on the surface area of NRVMs. β2a overexpression increased NRVM surface area and sarcomere organization. *: $p<0.05$ vs. AdGFP at the same MOI; **: $p<0.01$ vs. AdGFP at the MOI of 5.

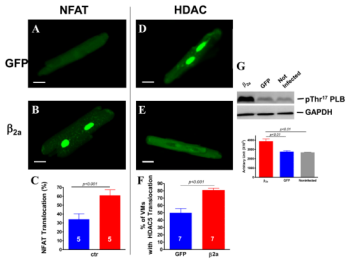

Figure 6. β2a overexpression induced translocation of NFAT3 and HDAC5 in cultured AFVMs

A & B, Examples of NFAT localization in GFP-VMs (**A**) or β2a-VMs (**B**). **C**, Averaged NFAT translocation rates in GFP-VMs and β2a-VMs. **D & E**, Examples of HDAC5 localization in AFVMs infected with AdGFP (**D**) or Adβ2a (**E**). **F**, Averaged HDAC5 translocation rates in GFP-VMs and β2a-VMs. **G**, Adβ2a significantly increased Thr17 phosphorylation on PLB. The bars in **A**, **B**, **D** and **E** are 15μm.

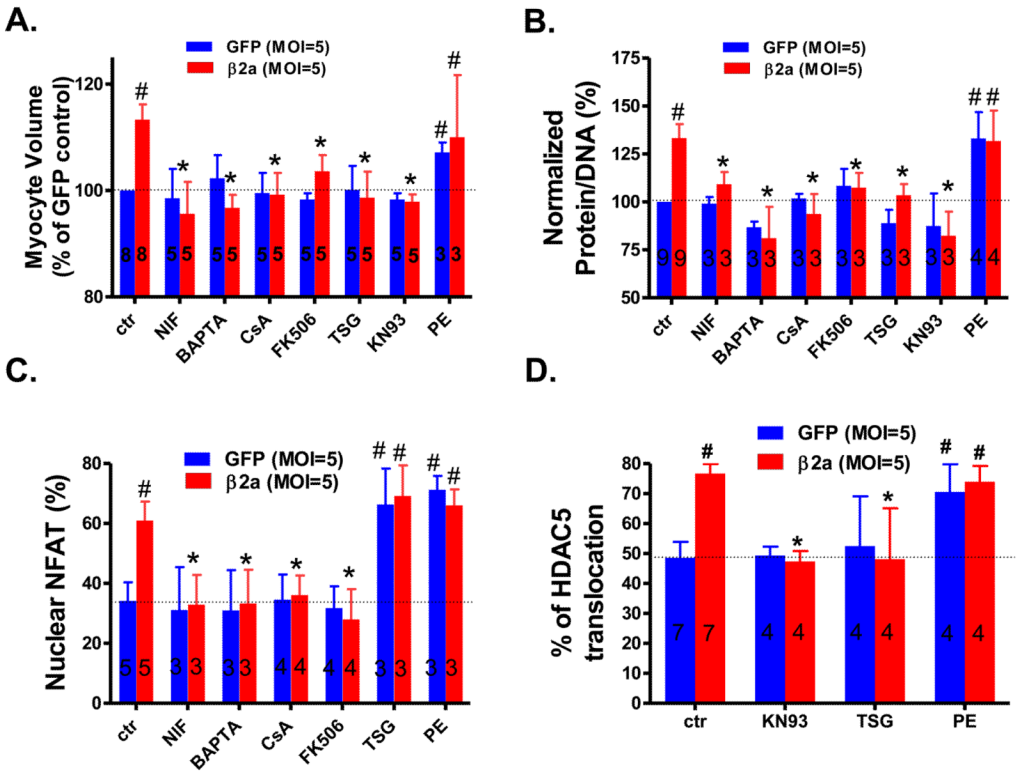

Figure 7. Effects of drugs on myocyte volume, protein/DNA ratio, NFAT and HDAC translocation in GFP- and β2a-AFVMs

Effects of a Cav1.2 blocker (nifedipine, 13μM), an intracellular Ca^{2+} chelator (BAPTA, 1μM), calcineurin (CaN) inhibitors (cyclosporine A, 5μM & FK506, 1μM), a SERCA inhibitor (thapsigargin (TSG), 10nM), a CaMK II inhibitor (KN93, 1μM) and a hypertrophy inducer (phenylephrine (PE), 10μM) on myocyte volume (**A**) and protein synthesis (**B**). The increases in myocyte volume (**A**) and protein/DNA ratio (**B**) were prevented by all drugs except PE. Nifedipine, BAPTA-AM, CsA and FK506 blocked NFAT translocation induced by β2a overexpression **(C).** KN93 and TSG prevented the increase of HDAC5 translocation induced by β2a overexpression but phenylephrine did not further increase HDAC5 translocation in β2a-VMs (**D**). $^{\#}$: $p<0.05$ vs. AdGFP without drug treatment; *: $p<0.05$ vs. β2a-VMs without drug treatment.

Table 1

Cavβ_{2a} grades $I_{Ca\text{-}L}$, contractions and Ca^{2+} transients in infected AFVMs

	NI	GFP (MOI=5)	GFP (MOI=100)	β2a (MOI=5)	β2a (MOI=100)	GFP (MOI=5) + TSG	β2a(MOI=5) + TSG
$I_{Ca\text{-}L}$ (pA/pF)	7.8±1.3, n=5	8.0±0.9, n=4	7.6±1.6, n=11	16.9±1.8, n=5$^{\%!@}$	23.4±2.7, n=10$^{\%!@}$	-	-
Fractional Shortening (%)	3.6±0.6, n=12	3.3±03, n=26	3.2±0.6, n=24	7.6±0.7, n=32$^{\%!@}$	9.8±1.2, n=28$^{\%!@}$	Not observed	Not observed
Resting cytosolic Ca^{2+} (410/480, indo-1)	0.73±0.06, n=35	0.73±0.05, n=28	0.75±0.02, n=38	0.71±0.05, n=38	0.69±0.03, n=38	0.81±0.03$^{!}$, n=10	0.81±0.02$^{!}$, n=11
Ca^{2+} transient amplitude (410/480)	0.82±0.02, n=35	0.82±0.03, n=28	0.84±0.03, n=38	0.95±0.06, n=38$^{\#\$\&}$	1.09±0.11, n=38$^{\#\$\&}$	Not observed	Not observed
Ca^{2+} transient amplitude (Δ410/480)	0.09±0.01, n=35	0.10±0.01, n=28	0.10±0.01, n=38	0.23±0.02, n=38$^{\#\$\&}$	0.40±0.13, n=38$^{\#\$\&}$	-	-
SR load (peak of caffeine induced Ca^{2+} transient, Δ410/480)	0.18±0.03, n=15	0.21±0.02, n=10	0.21±0.02, n=14	0.30±0.02, n=18	0.45±0.12, n=10	0.02±0.01$^{\$}$, n=10	0.03±0.01$^{\$}$, n=11
Fractional Ca^{2+} release (%)	50.0%	47.6%	47.6%	76.7%	88.9%	-	-

$^{\#}$*p<0.001* vs. noninfected;

$^{\$}$*p<0.001* vs. GFP (MOI=5);

$^{\&}$*p<0.001* vs. GFP (MOI=100)

$^{\%}$*p<0.05* vs. noninfected;

$^{!}$*p<0.05* vs. GFP (MOI=5);

$^{@}$*p<0.05* vs. GFP (MOI=100)

n: cells measured from at least 4 cultures